Screw-Theoretic Analysis Framework for Cooperative Payload Transport by Mobile Manipulator Collectives

Chin Pei Tang, *Student Member, IEEE*, Rajankumar M. Bhatt, *Student Member, IEEE*, Michel Abou-Samah, and Venkat Krovi, *Member, IEEE*

***Abstract*—In recent times, there has been considerable interest in creating and deploying modular cooperating collectives of robots. Interest in such cooperative systems typically arises when certain tasks are either too complex to be performed by a single agent or when there are distinct benefits that accrue by cooperation of many simple robotic modules. However, the nature of both the individual modules as well as their interactions can affect the overall system performance. In this paper, we examine this aspect in the context of cooperative payload transport by robot collectives wherein the physical nature of the interactions between the various modules creates a tight coupling within the system. We leverage the rich theoretical background of analysis of constrained mechanical systems to provide a systematic framework for formulation and evaluation of system-level performance on the basis of the individual-module characteristics. The composite multi-degree-of-freedom (DOF) wheeled vehicle, formed by supporting a common payload on the end-effectors of multiple individual mobile manipulator modules, is treated as an in-parallel system with articulated serial-chain arms. The system-level model, constructed from the twist- and wrench-based models of the attached serial chains, can then be systematically analyzed for performance (in terms of mobility and disturbance rejection). A two-module composite system example is used throughout the paper to highlight various aspects of methodical system model formulation, effects of selection of active, passive or locked articulations on system performance, and experimental validation on a hardware prototype test bed.**

***Index Terms*—Cooperative robotic system, in-parallel system, mobile manipulator, nonholonomic constraints, screw theory.**

I. Introduction

BIOLOGISTS who study animal aggregations such as swarms, flocks, school, and herds have observed the remarkable group-level cooperative achievement of tasks. For example, armies of ants leverage the collective strength and manipulation capabilities to move large food pieces, which would be impossible for a single ant. Thus, there is a considerable interest in engineering such teams/collectives of land-based mobile agents to achieve common goals in various application arenas from collective foraging to cooperative payload transport.

On one hand, deploying such teams of smaller simpler robot modules can yield significant benefits over deploying a single larger robot in terms of redundancy, robustness, and reliability. Other important benefits include capability for decentralization as well as ability to reconfigure to improve performance. On the other hand, such modularity creates challenges by way of increased choice of means to accomplish given tasks. In particular, in a modularly composed system, both the nature of the individual modules as well as their interactions can affect the overall system performance. Hence, a systematic (and preferably quantitative) framework for evaluation of the individual module- and system-level characteristics is desirable. This is an aspect that we examine in the context of cooperative payload transport by robot collectives in this paper.

Many of the entailed issues are highlighted in the illustrative example of household furniture movers moving a large piece of furniture. Traditionally, such movers employ variable numbers of modular wheeled dollies, as determined by the payload. These are positioned at suitable locations to ensure mobility, stability, and load distribution within the aggregation, which is then steered away as a single composite system. Occasionally, additional dollies may be added or the relative locations of existing dollies may be readjusted to avoid obstacles or to enhance overall performance. Thus, a fleet of semiautonomous wheeled modules that can cooperate to either assist the human operator or autonomously perform this overall payload transport process would have tremendous application in many material handling situations.

All our individual modules take the form of differentially driven wheeled mobile robots (WMR) with a mounted manipulator arm, as shown in Fig. 1(a). A composite multi-degree-of-freedom (DOF) wheeled vehicle is formed when a payload is placed at the end-effectors of multiple such modules. However, two or more WMRs, with rigid axles, cannot be arbitrarily coupled to each other due to the incompatibility of the velocities of the wheels. The potential degradation in the overall performance can range from loss of mobility, rattle-shake, unintentional compliance, wear and tear of the tires, and wheel slip. Hence, many approaches in the literature [1], [2] advocate the addition of further articulations between the various wheels/axles in order to accommodate the rigid body constraints, in our system this role is played by the mounted planar manipulator arm. The resulting

Manuscript received September 15, 2005; revised November 30, 2005. Recommended by Guest Editors, S. Agrawal and V. Krovi. This work was supported in part by the National Science Foundation CAREER Award under Grant IIS-0347653.

C. P. Tang, R. M. Bhatt, and V. Krovi are with the Department of Mechanical and Aerospace Engineering, State University of New York at Buffalo, Buffalo, NY 14260 USA (e-mail: chintang@eng.buffalo.edu; rmbhatt@eng.buffalo.edu; vkrovi@eng.buffalo.edu).

M. Abou-Samah was with the Center for Intelligent Machines, Department of Mechanical Engineering, McGill University, Montreal, QC H3A 2A7 Canada. He is now with the MSC Software Corporation, Ann Arbor, MI 48105 USA (e-mail: gishm@hotmail.com).

Digital Object Identifier 10.1109/TMECH.2006.871092

(a) (b)

Fig. 1. (a) Individual mobile manipulator module and (b) Composite system formed by 2 modules.

composite vehicle, of the form shown in Fig. 1(b), possesses: 1) the ability to accommodate changes in the relative configuration (by virtue of the compliant linkage); 2) a mechanism for detecting such changes (using sensed articulations); and 3) means to compensate for such disturbances (using the redundant actuation of the bases), while performing the payload transport task.

In general, a careful selection of the type, number, dimensions, and actuation of both the wheels attached to the base and the joints in the mounted manipulator are critical to determining the performance of the individual module. However, these aspects are examined elsewhere [3], [4] and yield the mobile manipulator configuration design shown in Fig. 1(a). Using this base module, it is our desire to create a composite vehicle that can be analyzed for performance in terms of mobility and disturbance rejection. In particular, we wish to address the following questions: 1) Can the system *accommodate* arbitrary payload motions? 2) Can the system *create* arbitrary payload motions? 3) Can the system *resist* arbitrary payload forces? and 4) What effect do various actuation schema have on payload manipulation performance?

To this end, we leverage the rich history and background of analysis methods for constrained articulated mechanical systems. In particular, a twist- and wrench-based analysis of in-parallel systems [5] provides the underlying framework for examining the performance of the cooperative system here. The unique contribution of this paper comes from: 1) the systematic modeling of the novel nonholonomic wheeled mobile manipulators; 2) systematic system-level motion- and force-capability analysis based on capabilities of the individual modules; 3) analysis of effects of selection of active/passive/locked articulation on payload transport performance; and 4) experimental verification of the disturbance accommodation, detection and compensation within the composite system.

This paper is organized as follows: Section II presents a brief overview of the pertinent literature. Twist-based modeling of the wheeled mobile manipulator module is introduced in Section III. In Section IV, the wrench system of the single mobile manipulator is determined with different actuation schemes. Section V analyzes the two-module cooperative system in detail. In Section VI, different actuation schemes are examined, followed by the experimental results in Section VII. Section VIII concludes the paper with brief discussions.

II. Background

Cooperative multirobot systems, ranging from multiple mobile robots [6], [7], to multiple manipulators [8], to multifingered hands [9], [10], and to multilegged vehicles [11], [12], have been extensively studied in a variety of contexts. We restrict our attention to cooperative physical manipulation by articulated wheeled mobile manipulators [13]–[17] focusing on the motion and force distribution issues.

Khatib *et al.* [13] developed a decentralized control structure for cooperative tasks with mobile manipulation systems with holonomic bases and fully actuated manipulators. Motion planning has also been considered for collaborating teams of nonholonomic mobile manipulators from various centralized perspectives [14], [15]. Kosuge *et al.* [16] proposed a simple method for carrying a large object by cooperation of multiple mobile manipulators with impedance based controllers by selectively locking and unlocking some joints of the mounted manipulators on mobile platforms. Yamakita *et al.* [17] implemented the passive velocity field control approach for the cooperative control of multiple mobile robots holding an object. In almost all these cases, the principal emphasis is on control of a system formed with generic wheeled mobile manipulator modules. Despite the significant influence on the overall system performance, typically scant attention is paid to the type, dimensions, or actuation of the wheels and articulations—a shortcoming that we address in this paper.

On a slightly different note, we also see that the composite system formed shares many features with the class of multi-degree-of-freedom (MDOF) wheeled vehicles [1], [18]–[23]. Some of these like the RollerRacer [18] and the Snakeboard [19] are case studies in underactuated locomotion. Several others like OMNIMATE/CLAPPER [1] and systems with multiple actively steered wheels [20]–[22] and WAAVS [23] feature redundancy in actuation. Several of these authors also note that despite gains in maneuverability over conventional mobile robots, the overconstrained nature with hybrid series-parallel kinematic chains creates challenges in design, planning, and control of such systems. The analysis methods adopted in this paper offer convenient tools for systematic system-level motion- and force-analysis based on the capabilities of the individual modules.

III. Twist Modeling of a Single Mobile Manipulator Module

We now briefly summarize the planar twist-based modeling of the articulated mechanical systems. An interested reader may refer Hunt [24] for the more traditional line-based screw-theoretic modeling. We, however, follow the approach presented in Murray *et al.* [25] and Selig [26]. The adopted twist- and wrench-modeling approach emphasizes the linkage to matrix-Lie group based modeling and analysis of rigid-body mechanics.

For a planar case, the relative configuration of a moving frame $\{E\}$ relative to a fixed frame $\{F\}$ is defined by the homogeneous transformation expressed in a 3×3 matrix form as

$$^{F}A_{E} = \begin{bmatrix} ^{F}R_{E} & ^{F}\underset{\sim}{d} \\ \underset{\sim}{0}^{T} & 1 \end{bmatrix} \tag{1}$$

where $^{F}R_{E} \in SO(2) = \{R \in \mathbb{R}^{2\times 2} : RR^{T} = I,\ \det R = +1\}$ is a rotation matrix and $^{F}\underset{\sim}{d} \in \mathbb{R}^{2}$ is a displacement vector. Thus, in a two-dimensional Euclidean task space, the configuration of a rigid body can be represented as an element of

$$^{F}A_{E} \in SE(2) = \left\{ A : A = \begin{bmatrix} R & \underset{\sim}{d} \\ \underset{\sim}{0}^{T} & 1 \end{bmatrix}, \underset{\sim}{d} \in \mathbb{R}^{2}, R \in SO(2) \right\}. \tag{2}$$

A twist matrix $T \in se(2)$ can be represented by a 3×3 matrix of the form

$$T = \begin{bmatrix} \Omega & \underset{\sim}{v} \\ \underset{\sim}{0}^{T} & 0 \end{bmatrix} \tag{3}$$

where $\Omega = \begin{bmatrix} 0 & -\omega \\ \omega & 0 \end{bmatrix} \in so(2)$ is a skew-symmetric matrix, $\omega \in \mathbb{R}$, and $\underset{\sim}{v} \in \mathbb{R}^{2}$. The twist vector then takes the form of $\underset{\sim}{t} = [\omega\ \ \underset{\sim}{v}^{T}]^{T} \in \mathbb{R}^{3}$. Note that ω is an angular velocity scalar and $\underset{\sim}{v}$ is a linear velocity vector in the plane. A body-fixed twist matrix corresponding to the motion of the moving frame $\{E\}$ with respect to its immediately preceding frame $\{F\}$ (as expressed in the moving frame $\{E\}$) can be formed as

$$^{E}\left[^{F}T_{E}\right] = \left[^{F}A_{E}^{-1}\right]\left[^{F}\dot{A}_{E}\right]. \tag{4}$$

Note that such a body-fixed twist description is particularly useful for the study of locomotion systems since it is invariant to the location of the inertial-fixed frame. The twist matrix can then be transformed to any arbitrary frame $\{N\}$ by a similarity transformation of

$$^{N}\left[^{F}T_{E}\right] = \left[^{N}A_{E}\right]{}^{E}\left[^{F}T_{E}\right]\left[^{N}A_{E}^{-1}\right]. \tag{5}$$

Alternatively, when considered in the twist vector form

$$^{N}\left[^{F}\underset{\sim}{t}_{E}\right] = \left[^{N}\Gamma_{E}\right]{}^{E}\left[^{F}\underset{\sim}{t}_{E}\right] \tag{6}$$

where the (twist) adjoint transform $[^{N}\Gamma_{E}]$ can be defined as

$$\left[^{N}\Gamma_{E}\right] = \begin{bmatrix} 1 & \underset{\sim}{0}^{T} \\ ^{N}[d_{y}\quad -d_{x}]^{T} & ^{N}R_{E} \end{bmatrix}. \tag{7}$$

A wrench $\underset{\sim}{w} = [\underset{\sim}{f}^{T}\ \ m]^{T} \in \mathbb{R}^{3}$ is an element of the dual vector space to the space of twists, where $\underset{\sim}{f}$ is the force vector in the plane and m is a scalar of pure moment. The reciprocity relationship $\circ$ between a wrench and a twist can be defined as

$$\underset{\sim}{w} \circ \underset{\sim}{t} = f_{x}v_{x} + f_{y}v_{y} + m_{z}\omega_{z} = 0 \tag{8}$$

and is nothing more than a statement of the Principle of Virtual Work. Finally, we note that wrenches as elements of the dual vector space to the space of twists transform between frames by way of the coadjoint (wrench adjoint) transform as

$$^{N}\left[^{F}\underset{\sim}{w}_{E}\right] = \left[^{N}\Gamma_{E}{}^{-1}\right]{}^{E}\left[^{F}\underset{\sim}{w}_{E}\right] = \left[^{N}\Gamma_{E}{}^{T}\right]{}^{E}\left[^{F}\underset{\sim}{w}_{E}\right]. \tag{9}$$

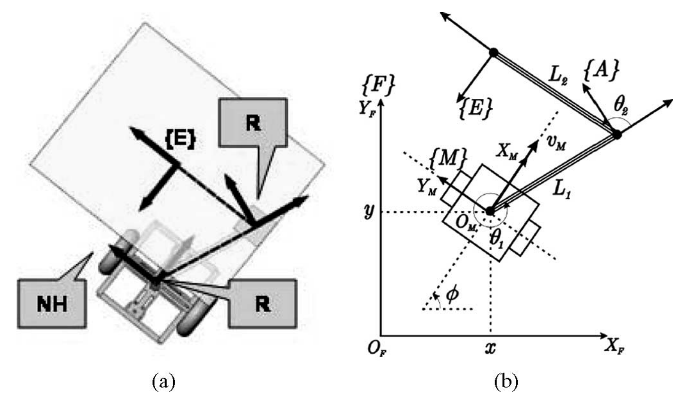

Fig. 2. Nonholonomic mobile manipulator (NH-RR) module (a) CAD model and (b) Corresponding schematic.

A. Modeling of Single Mobile Manipulator

Fig. 2 depicts a differentially-driven WMR with the base of a 2R manipulator mounted at the midpoint of the wheel axle (and denoted as a nonholonomic-revolute-revolute (NH-RR)-type mobile manipulator). The frame $\{M\}$ is rigidly attached to the center of the WMR, with the X_{M}-axis oriented in the direction of the forward travel of the mobile robot and the Y_{M}-axis oriented parallel to the direction of the nonholonomic constraint. Frame $\{A\}$ is rigidly attached at the distal joint of the first link. Frame $\{E\}$ is attached to the frame of reference of the payload. Thus, the second link is a "virtual link" that connects from the point of attachment of the manipulator with the payload to the payload reference frame. The configuration of the manipulator with the two revolute joints can be parameterized by the two relative angles θ_1 and θ_2, with the link lengths L_1 and L_2.

The kinematic model of the mobile manipulator is developed by composition of contributions from both the mobile platform and the manipulator. The twist of the mobile platform expressed in frame $\{M\}$, after factoring in the effect of nonholonomic constraint, can be written as

$$^{M}\left[^{F}T_{\mathrm{M}}\right] = {}^{M}\begin{bmatrix} 0 & 1 & 0 \\ -1 & 0 & 0 \\ 0 & 0 & 0 \end{bmatrix}\dot{\phi} + {}^{M}\begin{bmatrix} 0 & 0 & 1 \\ 0 & 0 & 0 \\ 0 & 0 & 0 \end{bmatrix} v_{\mathrm{M}} \tag{10}$$

where $\dot{\phi}$ and v_{M} are the angular and linear forward velocities of the mobile platform, respectively. The twists in (10) can be expressed in the payload frame $\{E\}$ by similarity transformation in (5). The manipulator twist can be expressed as a linear combination of the twist matrices of each DOF in the form of

$$^{E}\left[^{M}T_{E}\right] = {}^{E}\left[^{M}T_{A}\right]\dot{\theta}_{1} + {}^{E}\left[^{A}T_{E}\right]\dot{\theta}_{2}. \tag{11}$$

Finally, we express all the twists in the payload reference frame $\{E\}$ to construct the Jacobian matrix $\mathbf{J}$ as

$$^{E}\left[^{F}\underset{\sim}{t}_{E}\right] = \mathbf{J}\underset{\sim}{u} = [\underset{\sim}{t}_{1}\quad \underset{\sim}{t}_{2}\quad \underset{\sim}{t}_{3}\quad \underset{\sim}{t}_{4}]\begin{bmatrix} \dot{\phi} \\ v_{\mathrm{M}} \\ \dot{\theta}_{1} \\ \dot{\theta}_{2} \end{bmatrix} \tag{12}$$

where

$$\underset{\sim}{t}_1 = \begin{bmatrix} 1 \\ L_1 S_2 \\ L_1 C_2 + L_2 \end{bmatrix}, \quad \underset{\sim}{t}_2 = \begin{bmatrix} 0 \\ C_{12} \\ -S_{12} \end{bmatrix},$$

$$\underset{\sim}{t}_3 = \begin{bmatrix} 1 \\ L_1 S_2 \\ L_1 C_2 + L_2 \end{bmatrix}, \quad \underset{\sim}{t}_4 = \begin{bmatrix} 1 \\ 0 \\ L_2 \end{bmatrix}$$

and $S_{ab\cdots} = \sin(\theta_a + \theta_b + \cdots)$ and $C_{ab\cdots} = \cos(\theta_a + \theta_b + \cdots)$.

Depending on the context, the columns of the Jacobian matrix $\mathbf{J}$ can be interpreted as the vector fields spanning the distribution of feasible twists. In the remainder of the paper, we denote the end-effector twist ${}^E\underset{\sim}{t}$ instead of ${}^E[{}^F\underset{\sim}{t}_E]$.

B. Twist Distribution-Based Analysis

An arbitrary end-effector twist ${}^E\underset{\sim}{t}$ is considered feasible if it lies within the span of the distribution $\mathbf{J}$. Conceptually, one could perform this check by determining the rank of the augmented matrix

$$\mathbf{G} = [\mathbf{J} \quad {}^E\underset{\sim}{t}]. \tag{13}$$

If $\operatorname{rank}(\mathbf{G}) = \operatorname{rank}(\mathbf{J})$, then ${}^E\underset{\sim}{t}$ lies in the span of the distribution $\mathbf{J}$. While this method allows *post-facto verification*, it offers no guidance in determining the conditions under which an arbitrary twist ${}^E\underset{\sim}{t}$ is guaranteed to lie in the span of $\mathbf{J}$.

Hence, we prefer to use the alternate constructive method, which begins by determining the set of reciprocal wrenches that span the constraint codistribution that annihilates the vector fields in $\mathbf{J}$. Any candidate end-effector twist ${}^E\underset{\sim}{t}$ lying in the span of the vector fields of $\mathbf{J}$ would also have to be annihilated completely by the reciprocal wrenches [25].

We note that the vector fields of the complete distribution $\mathbf{J}$ can be partitioned into an active distribution $\mathbf{J}_\mathrm{a}$ due to the actuated joints and a passive distribution $\mathbf{J}_\mathrm{p}$ due to the passive joints. Typically, we seek to create the end-effector twist using only the controllable vector fields of the active distribution. However, there may exist cases where an end-effector twist is not spanned by the active distribution and requires the contribution from the passive distribution.

In the mobile manipulators under consideration, we always consider the base to be actuated, which ensures a $\mathbf{J}_\mathrm{a}$ of rank at least 2. The actuation of at least one of the mounted manipulator joints then can potentially create a full rank $\mathbf{J}_\mathrm{a}$. However, analyzing the more restrictive case with active mobile base and passive mounted manipulator joints is also instructive. In this case, the end-effector twist can be decomposed into

$${}^E\underset{\sim}{t} = \mathbf{J}_\mathrm{a}\underset{\sim}{u}_\mathrm{a} + \mathbf{J}_\mathrm{p}\underset{\sim}{u}_\mathrm{p} \tag{14}$$

where $\underset{\sim}{u}_\mathrm{a} = [\dot{\phi} \quad v_\mathrm{M}]^T, \quad \underset{\sim}{u}_\mathrm{p} = [\dot{\theta}_1 \quad \dot{\theta}_2]^T$,

$$\mathbf{J}_\mathrm{a} = \begin{bmatrix} 1 & 0 \\ L_1 S_2 & C_{12} \\ L_1 C_2 + L_2 & -S_{12} \end{bmatrix}, \quad \mathbf{J}_\mathrm{p} = \begin{bmatrix} 1 & 1 \\ L_1 S_2 & 0 \\ L_1 C_2 + L_2 & L_2 \end{bmatrix}.$$

An arbitrary end-effector twist can be first projected onto the active distribution $\mathbf{J}_\mathrm{a}$ in order to determine active actuator rates $\underset{\sim}{u}_\mathrm{a}$. In the absence of an exact solution, the remnants may also be projected onto the passive distribution $\mathbf{J}_\mathrm{p}$ to determine $\underset{\sim}{u}_\mathrm{p}$. The reciprocal wrench $\underset{\sim}{w}_\mathrm{a}$ to all the twists in the active distribution $\mathbf{J}_\mathrm{a}$ can be determined as

$$\underset{\sim}{w}_\mathrm{a} = \left[\frac{S_{12}}{C_{12}} \quad 1 \quad \left(\frac{-L_1 C_1}{C_{12}} - L_2\right)\right]^T \tag{15}$$

where $\underset{\sim}{w}_\mathrm{a} \circ \mathbf{J}_\mathrm{a} = 0$, and it is guaranteed to be reciprocal to any twist that lies in the span of the distribution $\mathbf{J}_\mathrm{a}$. Hence, for an arbitrary end-effector twist ${}^E\underset{\sim}{t} = [\omega_{Ez} \;\; v_{Ex} \; v_{Ey}]^T$ to lie in this distribution, the reciprocity requirement yields the condition

$$[-L_1 C_1 - L_2 C_{12}]\omega_{Ez} + [S_{12}]v_{Ex} + [C_{12}]v_{Ey} = 0. \tag{16}$$

We note that a twist ${}^E\underset{\sim}{t}$ applied to the end-effector would naturally create a helicoidal velocity vector field (that corresponds to rigid motions of all attached points) that can be expressed in frame $\{M\}$ as

$${}^M[{}^E\underset{\sim}{t}] = \begin{bmatrix} \omega_{Ez} \\ [L_1 S_1 + L_2 S_{12}]\omega_{Ez} + C_{12}v_{Ex} - S_{12}v_{Ey} \\ [-L_1 C_1 - L_2 C_{12}]\omega_{Ez} + S_{12}v_{Ex} + C_{12}v_{Ey} \end{bmatrix}. \tag{17}$$

In light of (17), we see that the condition in (16) is nothing more than the requirement that the Y_M-component of the helicoidal velocity vector field in the mobile robot frame $\{M\}$ be identically zero. This can be easily achieved by aligning the forward direction of travel (the X_M-axis of the robot) with the helicoidal velocity field. Thus, this simple strategy guarantees that any arbitrary end-effector twist ${}^E\underset{\sim}{t}$ lies within the span of the active distributions $\mathbf{J}_\mathrm{a}$ alone and is employed for analysis and control of our system in subsequent sections.

However, we note that disturbances may cause the system to drift away from this preferred configuration, where the ${}^E\underset{\sim}{t}$ lies in the span of the active distributions. In such cases, we need to ensure that any arbitrary ${}^E\underset{\sim}{t}$ can then be accommodated within the combined distribution. A simple check verifies that the set of reciprocal wrenches to the complete distribution $\mathbf{J}$ is in fact the null set.

IV. Wrench Modeling of a Single Mobile Manipulator Module

The total wrench ${}^E\underset{\sim}{w}$ that can be applied or actively equilibrated at the end-effector lies in the span of the set of wrenches created by all actuated joints

$${}^E\underset{\sim}{w} = \sum_{k=1}^{N_\mathrm{a}} \underset{\sim}{w}_k c_k = \mathbf{W}\underset{\sim}{c}, \quad \forall \underset{\sim}{w}_k \in \{\text{active wrenches}\} \tag{18}$$

where N_a is the number of actuated joints and c_k is the wrench intensity of the kth actuated joint. For individual mobile manipulators, the end-effector wrench system can be systematically developed on the basis of reciprocity relationships. Given a twist system $\{\underset{\sim}{t}_1, \underset{\sim}{t}_2, \ldots, \underset{\sim}{t}_n\}$, the wrench contribution due to actuation of the kth joint can be determined using the method of

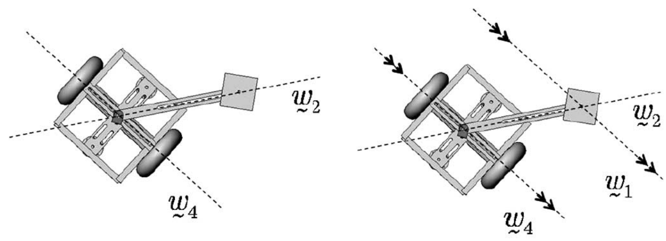

(a) (b)

Fig. 3. Lines of action of wrench of single mobile manipulator module for (a) A-PP actuation scheme and (b) A-LP actuation scheme.

selectively non-reciprocal screws (SRNS) [5], [27] as

$$\begin{aligned} &\underset{\sim}{w}_k \circ \underset{\sim}{t}_k \neq 0 \\ &\underset{\sim}{w}_k \circ \underset{\sim}{t}_j = 0, \forall j = 1, \ldots, k-1, k+1, \ldots, n. \end{aligned} \tag{19}$$

In our work, we also wish to consider the role of different actuation schema and denote active joints as A, passive joints as P, and locked joints as L. For each NH-RR module, we denote the overall actuation scheme by a triple. The first alphabet corresponds to the actuation of the nonholonomic base, second and third alphabets represent the actuation of the first (θ_1) and second (θ_2) joints of the manipulator, respectively. For instance, A-LP represents the actuation scheme with nonholonomic base active, first joint held locked but second joint held passive. In the rest of this section, we develop the set of wrenches for two particular actuation schema: (a) A-PP and (b) A-LP. Other possibilities are listed in the Appendix.

A. A-PP Actuation Scheme

For the A-PP actuation scheme, the end-effector twist is the span of all four twists as shown in (12). Hence, the instantaneous selectively non-reciprocal wrenches can be determined as

$$\begin{aligned} &\underset{\sim}{w}_1 = \emptyset, \quad \underset{\sim}{w}_2 = \begin{bmatrix} -\frac{C_2}{S_2} \\ 1 \\ -L_2 \end{bmatrix}, \quad \underset{\sim}{w}_3 = \emptyset, \\ &\underset{\sim}{w}_4 = \begin{bmatrix} \frac{S_{12}}{C_{12}} \\ 1 \\ \frac{-L_1 C_1}{C_{12}} - L_2 \end{bmatrix} \end{aligned} \tag{20}$$

where $\emptyset$ is a null set. Each non-null wrench also has a geometric interpretation as the line of action of a pure force [see $\underset{\sim}{w}_2$ and $\underset{\sim}{w}_4$ in Fig. 3(a)]. However, since only the mobile base is actuated, any actively equilibrated wrench must lie in the span of $\{\underset{\sim}{w}_1, \underset{\sim}{w}_2\}$.

B. A-LP Actuation Scheme

Locked joints do not contribute to the end-effector twist system and hence must be treated carefully. For the A-LP actuation scheme, the total twist becomes

$$^{E}\underset{\sim}{t} = [\underset{\sim}{t}_1 \quad \underset{\sim}{t}_2 \quad \underset{\sim}{t}_4] \begin{bmatrix} \dot{\phi} \\ v_M \\ \dot{\theta}_2 \end{bmatrix}. \tag{21}$$

Thus, the instantaneous selectively nonreciprocal wrenches of this case are

$$\begin{aligned} &\underset{\sim}{w}_1 = \begin{bmatrix} \frac{S_{12}}{C_{12}} \\ 1 \\ -L_2 \end{bmatrix}, \quad \underset{\sim}{w}_2 = \begin{bmatrix} -\frac{C_2}{S_2} \\ 1 \\ -L_2 \end{bmatrix}, \\ &\underset{\sim}{w}_4 = \begin{bmatrix} \frac{S_{12}}{C_{12}} \\ 1 \\ \frac{-L_1 C_1}{C_{12}} - L_2 \end{bmatrix}. \end{aligned} \tag{22}$$

Fig. 3(b) depicts the lines of actions of the wrenches $\underset{\sim}{w}_1, \underset{\sim}{w}_2, \underset{\sim}{w}_4$ for the module with an A-LP actuation scheme. Here the active wrenches must lie in the span of $\{\underset{\sim}{w}_1, \underset{\sim}{w}_2\}$.

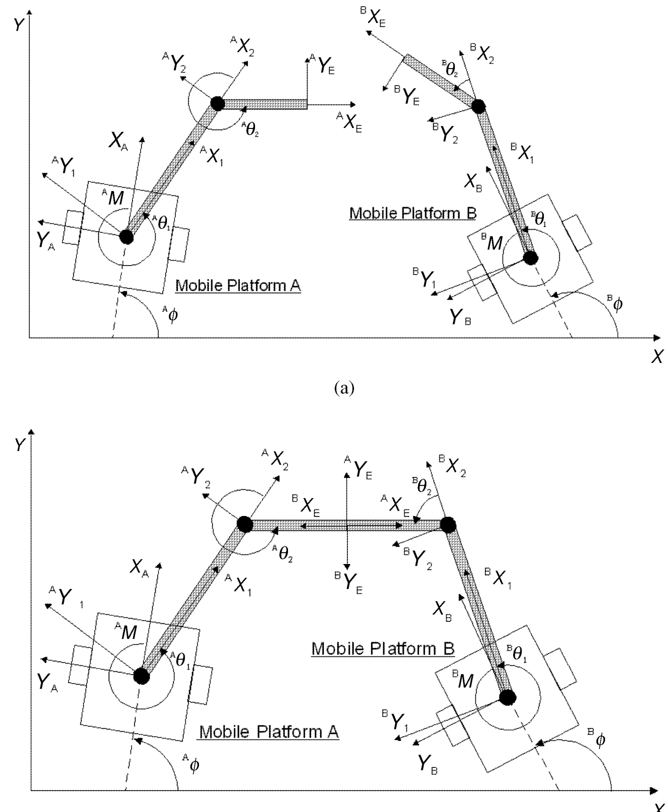

(a)

(b)

Fig. 4. Overall system considered as (a) independent mobile manipulators; or (b) composite system.

V. Cooperative System Analysis

In this section, we consider the collaboration between two NH-RR-type mobile manipulator modules carrying a common payload as shown in Fig. 4. The end-effectors of the physical manipulators are assumed to be rigidly attached to the payload. The locations of the attachments of these fixture sites are also assumed to be known *a priori*. A frame attached to a point of interest on the common payload is treated as the end-effector frame of the two flanking mobile manipulator systems [see Fig. 4(a)]. In doing so, the individual modules may be treated as the serial-chain legs/arms of an in-parallel mechanism [see Fig. 4(b)].

The ability of the in-parallel/composite system to accommodate arbitrary twist disturbance or create arbitrary end-effector twist is completely characterized by examining the twists within each serial chain and is considered elsewhere [28]. However, in order to analyze the force capabilities of the composite system, we need to consider the wrench contributions of all the modules of the in-parallel system [29].

The resultant wrench ${}^E\underset{\sim}{w}$ of an in-parallel mechanism must lie in the span of the end-effector wrenches of all the individual serial chains. Let $\underset{\sim}{w}_k^i$ be the instantaneous wrench applied by the serial chain i when the k th joint is actuated. Thus

$$ {}^E\underset{\sim}{w} = \mathbf{W}\,\underset{\sim}{c} \tag{23} $$

where $\mathbf{W} = \text{column}(\underset{\sim}{w}_k^i)$, for $k = 1, \ldots, N_a$ (number of active DOF. within the ith chain) and $i = 1, \ldots, N_b$ (number of chains), and $\underset{\sim}{c}$ is the vector of corresponding wrench intensities. For non-redundant actuation, $\mathbf{W}$ is a square matrix and if it is nonsingular, the unknown vector of resultant forces can be calculated as

$$ \underset{\sim}{c} = [\mathbf{W}^{-1}]\,{}^E\underset{\sim}{w}. \tag{24} $$

However, more typically, the equilibrium equation in (23) tend to be indeterminate since $\mathbf{W}$ possesses more columns than rows. A variety of methods have been proposed in the literature to resolve such redundancy as frequently done in multilegged walkers [30], multifingered hands [9], and multiarm systems [31]. We restrict the scope of this paper to ensuring that an arbitrary end-effector wrench lies within the span of the individual active wrenches contributed from the various chains.

However, in some cases, the rank of the system wrench matrix $\mathbf{W}$ is less than the task dimension, despite the presence of surplus actuation. The implication is that in such cases an arbitrary wrench does not lie in the span of the actuated wrench set. This results in the undesired case of a force-unconstrained in-parallel system and is examined in greater detail in the case studies.

Alternatively, an existing wrench system could lose rank at special (singular) configurations creating an instantaneously force-unconstrained in-parallel system. In such cases, the singularity of such system can be determined by determining the conditions under which all $n \times n$ submatrices of $\mathbf{W}$ (where $n =$ dimension of task space) are singular [32]. However, the presence of such singularities within the workspace is a rarer occurrence [33] and is not examined here.

VI. Case Studies

A. *Cooperation Between Modules With A-PP and A-PP Actuation Schema*

To begin with, we consider the case of two modules with A-PP actuation schema, i.e. the articulations on both mounted manipulators are passive. The combined wrench system, in this case, can be written as

$$ {}^E\underset{\sim}{w} = \mathbf{W}\,\underset{\sim}{c} = \begin{bmatrix} \underset{\sim}{w}_1^A & \underset{\sim}{w}_2^A & \bar{\underset{\sim}{w}}_1^B & \bar{\underset{\sim}{w}}_2^B \end{bmatrix} \begin{bmatrix} c_1^A \\ c_2^A \\ \bar{c}_1^B \\ \bar{c}_2^B \end{bmatrix} \tag{25} $$

where, taking $\{E^A\}$ as the reference payload frame $\{E\}$

$$ \begin{aligned} {}^E\left[\bar{\underset{\sim}{w}}_i^B\right] &= \left[{}^E\Gamma_{E^B}^T\right]\,{}^{E^B}\left[\underset{\sim}{w}_i^B\right], \\ \left[{}^E\Gamma_{E^B}^T\right] &= \begin{bmatrix} 1 & 0 & 0 \\ 0 & -1 & 0 \\ 0 & 0 & -1 \end{bmatrix} \end{aligned} \tag{26} $$

and $\left[{}^E\Gamma_{E^B}^T\right]$ is the coadjoint transform. Nominally, from the viewpoint of actuation the system appears to be redundant since there are four active wrenches available to span the planar task-wrench space. However, given that, in this case

$$ \begin{aligned} &w_1^A = \emptyset, \quad \underset{\sim}{w}_2^A = \begin{bmatrix} -\frac{C_2^A}{S_2^A} \\ 1 \\ -L_2^A \end{bmatrix}, \quad \bar{w}_1^B = \emptyset \\ &\bar{\underset{\sim}{w}}_2^B = \begin{bmatrix} -\frac{C_2^B}{S_2^B} \\ -1 \\ L_2^B \end{bmatrix}. \end{aligned} \tag{27} $$

$$ \mathbf{W} = \begin{bmatrix} -\frac{C_2^A}{S_2^A} & -\frac{C_2^B}{S_2^B} \\ 1 & -1 \\ -L_2^A & L_2^B \end{bmatrix} \tag{28} $$

this combined wrench system only has rank 2 since $\underset{\sim}{w}_1^A$ and $\bar{\underset{\sim}{w}}_1^B$ are null sets. This constitutes a force-unconstrained wrench system since only special wrenches that lie in the span of $\underset{\sim}{w}_2^A$ and $\bar{\underset{\sim}{w}}_2^B$ can be exactly equilibrated. This also implies existence of a payload twist system of dimension 1. In lay terms, a mobile superstructure is formed atop the wheeled bases, which does not allow the relative position of the payload to be fixed with respect to the wheeled bases.

Geometrically, this may be visualized as follows: the lines of actions of pure force wrenches $\underset{\sim}{w}_2^A$ and $\bar{\underset{\sim}{w}}_2^B$ always intersect at a common point and the system is now unable to resist any pure moment applied about this point (see Fig. 5). To improve the situation, one can consider an NH-RR system with first joint locked in Module A as considered next.

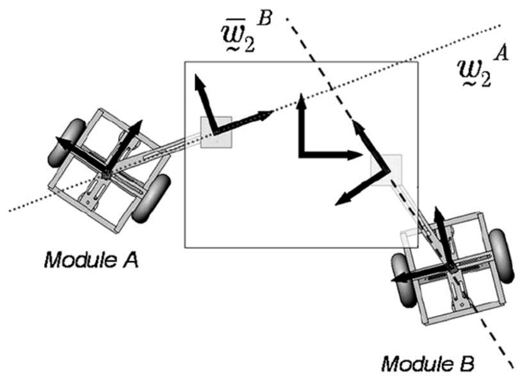

Fig. 5. Lines of action of wrenches of two collaborative modules with A-PP actuation schemes.

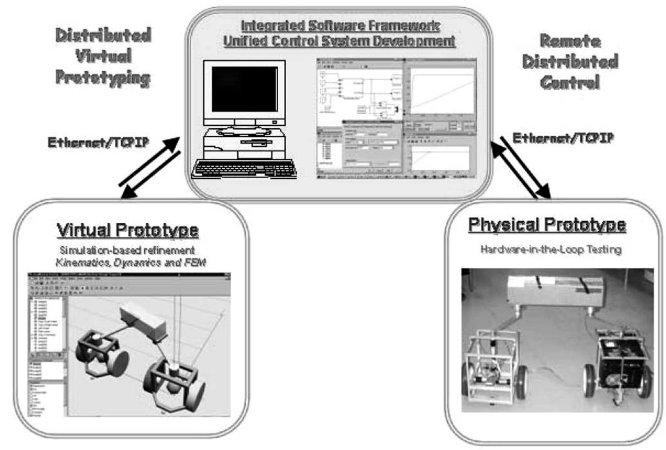

Fig. 6. Paradigm for development and testing of the control scheme.

B. Cooperation Between Modules With A-LP and A-PP Actuation Schema

In this case, if Module A is A-LP and Module B is A-PP, the combined system can be written as

$$ {}^{E}\underset{\sim}{w} = \mathbf{W}\,\underset{\sim}{c} = \begin{bmatrix} \underset{\sim}{w}_1^A & \underset{\sim}{w}_2^A & \bar{\underset{\sim}{w}}_1^B & \bar{\underset{\sim}{w}}_2^B \end{bmatrix} \begin{bmatrix} c_1^A \\ c_2^A \\ \bar{c}_1^B \\ \bar{c}_2^B \end{bmatrix} \tag{29} $$

where

$$ \underset{\sim}{w}_1^A = \begin{bmatrix} \frac{S_{12}^A}{C_{12}^A} \\ 1 \\ -L_2^A \end{bmatrix}, \quad \underset{\sim}{w}_2^A = \begin{bmatrix} -\frac{C_2^A}{S_2^A} \\ 1 \\ -L_2^A \end{bmatrix}, $$

$$ \bar{\underset{\sim}{w}}_1^B = \emptyset, \quad \bar{\underset{\sim}{w}}_2^B = \begin{bmatrix} -\frac{C_2^B}{S_2^B} \\ -1 \\ L_2^B \end{bmatrix} \tag{30} $$

$$ \mathbf{W} = \begin{bmatrix} \frac{S_{12}^A}{C_{12}^A} & -\frac{C_2^A}{S_2^A} & -\frac{C_2^B}{S_2^B} \\ 1 & 1 & -1 \\ -L_2^A & -L_2^A & L_2^B \end{bmatrix}. \tag{31} $$

The rank of this matrix is in general 3 (nonsingular) and thus the system is capable of resisting arbitrary instantaneous disturbance forces/moments. Any singularity of this system wrench matrix is configuration dependent, which can be determined by considering the singularities of the various full-rank submatrices [34]. We do not report the singularity analysis in this paper but reiterate some general observations about singularities arising in in-parallel systems. For example, each module can individually become singular, but this may be detected and avoided by monitoring the individual chain Jacobian matrices. Similarly, a system-level singularity may arise when multiple such modules become singular simultaneously, when the rank of the system wrench matrix drops below 3, which is a rare occurrence [33].

Finally, we note that while we use this system configuration for the experimental testing, other alternatives also exist, such as locking second joint in Module A, or locking both joints in Module A, or locking the corresponding joints of Module B.

VII. Experimental Setup and Evaluation

We examined experimental verification of capabilities for disturbance accommodation, detection, and compensation in a composite system of cooperating modules with the A-LP and A-PP actuation schema. Details of the design, analysis, physical prototyping, controller design, and ultimately experimental validation of a hardware-in-the-loop test bed consisting of a system of two cooperating mobile manipulators are available in [3], [28], and [35]. We briefly summarize the key aspects next in this section while providing focused references.

Our paradigm for rapid development, refinement, and implementation of system design emphasizes: 1) development of the control scheme in a user-friendly graphical high-level block diagrammatic language; 2) simulation, testing, and refinement of the control system by virtual prototyping; and 3) rapid conversion of the refined control system into a form suitable for real-time execution on an embedded controller for hardware-in-the-loop testing, as shown in Fig. 6.

In focusing on payload transport in a quasi-static setting, we prescribe the motion of the payload frame along a straight line trajectory with a forward velocity of 2.54 cm/s and zero angular velocity. Fig. 7 depicts the nominal desired relative configuration of the overall system with frames $\{M\}$ of Module A and Module B initially aligned in the same direction but offset by a distance of 62 cm in the Y-direction. Each NH-RR module is controlled using an online planning method described in [28]. The control is accomplished using a bilevel hierarchical scheme with an upper level design of steerable vector fields and a lower level stabilizing controller for the NH-RR-type mobile manipulator. The implemented decentralized planning scheme

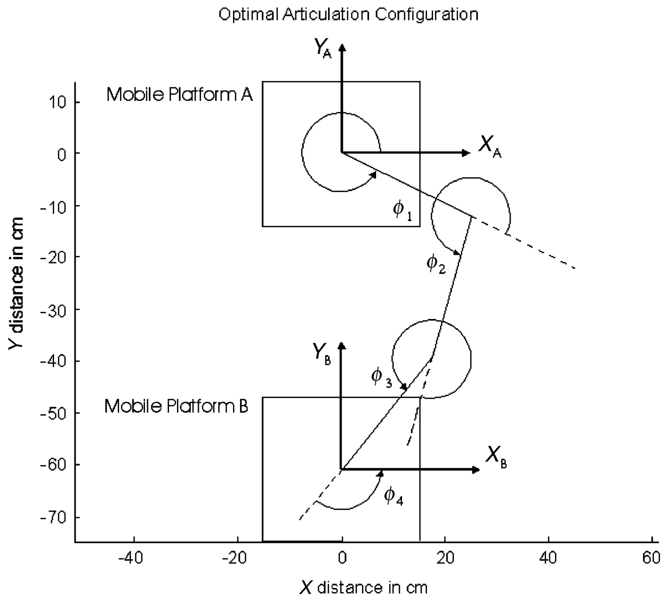

Fig. 7. Initial configuration of the composite system of two NH-RRs.

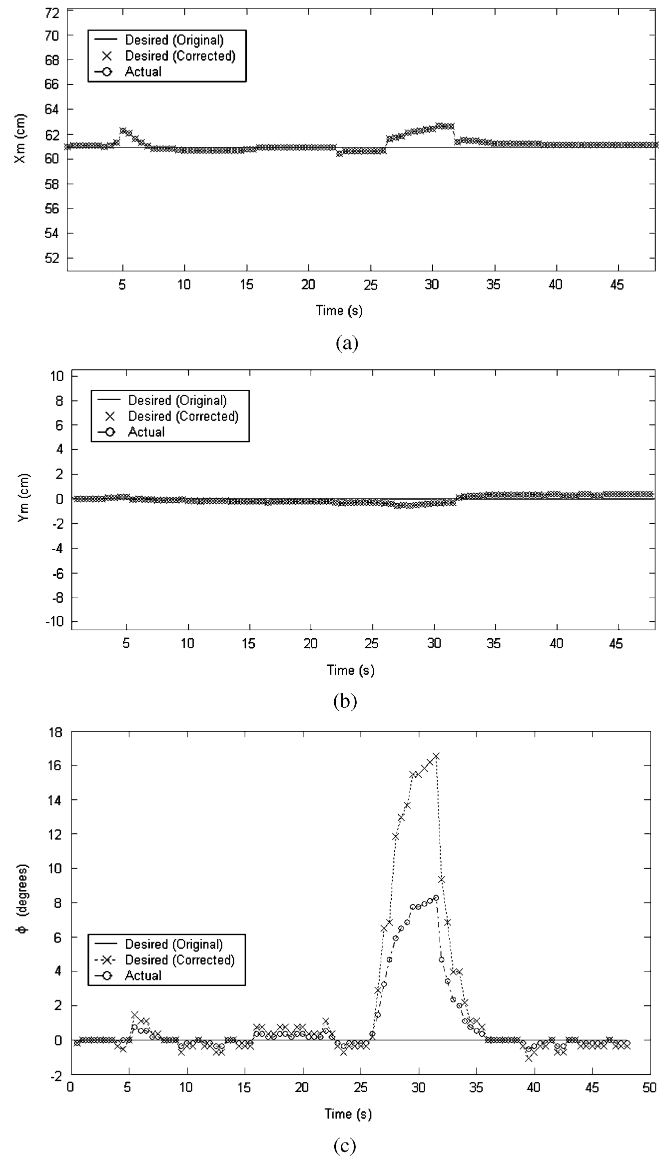

Fig. 8. Articulation based estimation of position and orientation differences between frames $\{M\}$ of Modules A and B used for the decentralized control.

for modules uses the online measurements from the articulations in the control.[1]

A significant disturbance to the relative configuration of the system is introduced by causing the left wheels of Module A to run over a small bump. As seen in Fig. 8, the online planning scheme is able to detect errors in the relative configuration as well as correct it to restore the desired configuration. In Fig. 8(a)–(c), the Desired (Original) (— line) is the nominal desired trajectory that was computed offline; the Desired (Corrected) (– × – line) is the desired trajectory resulting from the online sensor-based computation that deviates from the nominal desired trajectory in response to the changed relative configuration; Actual (– ○ – line) is the actual trajectory followed by the system as determined by postprocessing the measurements of the instrumented articulations.

Note, however, that while the relative system configuration is maintained, errors relative to a global reference frame cannot be detected if both mobile bases undergo identical simultaneous disturbances. Detection of such absolute errors would require external references and is not considered here.

VIII. Conclusion

In this paper, we examined the use of screw-theoretic analysis tools to provide a systematic framework for formulation and evaluation of system-level performance of a cooperative payload transport task by a modularly composed system of multiple wheeled mobile manipulators. Specifically, we examined the systematic modeling of the novel nonholonomic wheeled mobile manipulator modules (which form the serial-chain arms/legs); the systematic assembly of the in-parallel composite system model and subsequent analysis of the effects of selection of the actuation at the articulations (active, passive, or locked) on system performance. In particular, by analyzing a two-module composite system, we illustrated how a marginal change in the selection of actuation within the system can significantly affect the overall performance. The analysis also led to the selection of a candidate system configuration capable of accommodating and correcting motion and force-disturbances applied at the payload which was then validated experimentally. The overall framework employed here may also be easily extended to treat larger composite system implementations with more mobile manipulator modules.

Appendix

Table I lists the set of selectively non-reciprocal wrenches that arise for each of the nine cases of all possibilities of actuation schema for the NH-RR module (with the assumption that the mobile base is always actuated). Note that this computation

[1] Videos of experimental evaluation are available at http://mechatronics.eng.buffalo.edu/research/mobilemanipulator.

TABLE I
INSTANTANEOUS SELECTIVELY NON-RECIPROCAL WRENCH SYSTEMS OF AN INDIVIDUAL NH-RR WITH VARIOUS POSSIBLE ACTUATION SCHEMA (A = ACTUATED, P = PASSIVE, L = LOCKED) WITH NH JOINT ALWAYS ACTUATED

Case	Instantaneous wrenches
A-PP A-PA A-AP A-AA	$\underset{\sim}{w}_1 = \varnothing,\ \underset{\sim}{w}_2 = \begin{bmatrix} -\dfrac{C_2}{S_2} \\ 1 \\ -L_2 \end{bmatrix},\ \underset{\sim}{w}_3 = \varnothing,\ \underset{\sim}{w}_4 = \begin{bmatrix} \dfrac{S_{12}}{C_{12}} \\ 1 \\ \dfrac{-L_1 C_1}{C_{12}} - L_2 \end{bmatrix}$
A-LP A-LA	$\underset{\sim}{w}_1 = \begin{bmatrix} \dfrac{S_{12}}{C_{12}} \\ 1 \\ -L_2 \end{bmatrix},\ \underset{\sim}{w}_2 = \begin{bmatrix} -\dfrac{C_2}{S_2} \\ 1 \\ -L_2 \end{bmatrix},\ \underset{\sim}{w}_4 = \begin{bmatrix} \dfrac{S_{12}}{C_{12}} \\ 1 \\ \dfrac{-L_1 C_1}{C_{12}} - L_2 \end{bmatrix}$
A-PL A-AL	$\underset{\sim}{w}_1 = \underset{\sim}{w}_3 = \begin{bmatrix} \dfrac{S_{12}}{C_{12}} \\ 1 \\ \dfrac{-L_1 C_1}{C_{12}} - L_2 \end{bmatrix},\ \underset{\sim}{w}_2 = \begin{bmatrix} 1 & 0 \\ 0 & 1 \\ -L_1 S_2 & -L_1 C_2 - L_2 \end{bmatrix}$
A-LL	$\underset{\sim}{w}_1 = \begin{bmatrix} \dfrac{S_{12}}{C_{12}} & 0 \\ 1 & 0 \\ 0 & 1 \end{bmatrix},\ \underset{\sim}{w}_2 = \begin{bmatrix} 1 & 0 \\ 0 & 1 \\ -L_1 S_2 & -L_1 C_2 - L_2 \end{bmatrix}$

depends solely on the twist system available at the end-effector and does not consider the actuation status of the joints. This actuation status comes into play when the end-effector wrench system is created and now reflects the net end-effector wrench system composed as the span of the selectively non-reciprocal wrenches of the active joints. Finally, we note that the system wrench matrix can be generated by transforming all the end-effector wrench systems to a common payload frame using the coadjoint transformation in (9).

REFERENCES

[1] J. Borenstein, B. Everett, and L. Feng, *Navigating Mobile Robots: Systems and Techniques*. Wellesley, MA: A. K. Peters, 1996.

[2] J. Borenstein, H. R. Everett, L. Feng, and D. Wehe, "Mobile robot positioning: Sensors and techniques," *J. Robot. Syst.*, vol. 14, pp. 231–249, 1997.

[3] M. Abou-Samah, "A kinematically compatible framework for collaboration of multiple non-holonomic wheeled mobile robots," M.S. thesis, Dept. Mech. Eng. Center Intell. Mach., McGill Univ., Montreal, Canada, 2001.

[4] M. Abou-Samah and V. Krovi, "Optimal configuration selection for a cooperating system of mobile manipulators," presented at the 2002 ASME Design Eng. Tech. Conf., Montreal, QC, Canada, 2002.

[5] S. K. Agrawal and B. Roth, "Statics of in-parallel manipulators," *J. Mech. Design, Trans. ASME*, vol. 114, pp. 564–568, 1992.

[6] R. C. Arkin and G. A. Bekey, *Robot Colonies*. Boston: Kluwer, 1997.

[7] Y. Cao, A. S. Fukunaga, and A. B. Kahng, "Cooperative mobile robotics: Antecedents and directions," *Auton. Robots*, vol. 4, pp. 7–27, 1997.

[8] A. J. Koivo and G. A. Bekey, "Report of workshop on coordinated multiple robot manipulators: Planning, control, and application," *IEEE Trans. Robot. Autom.*, vol. 4, no. 1, pp. 91–93, Feb. 1988.

[9] J. Kerr and B. Roth, "Analysis of multifingered hands," *Int. J. Robot. Res.*, vol. 4, pp. 3–17, 1986.

[10] J. K. Salisbury and J. J. Craig, "Articulated hands: Force control and kinematic issues," *Int. J. Robot. Res.*, vol. 1, pp. 4–17, 1982.

[11] V. Kumar and K. J. Waldron, "Force distribution in closed kinematic chains," *IEEE Trans. Robot. Autom.*, vol. 4, no. 6, pp. 657–664, Dec. 1988.

[12] S. M. Song and K. J. Waldron, *Machines That Walk*. Cambridge, MA: MIT Press, 1989.

[13] O. Khatib, K. Yokoi, K. Chang, D. Ruspini, R. Holmberg, and A. Casal, "Vehicle/arm coordination and multiple mobile manipulator decentralized cooperation," presented at the 1996 IEEE/RSJ Int. Conf. Intelligent Robots Syst., Osaka, Japan, 1996.

[14] J. Desai and V. Kumar, "Motion planning for cooperating mobile manipulators," *J. Robot. Syst.*, vol. 10, pp. 557–579, 1999.

[15] H. G. Tanner, K. J. Kyriakopoulos, and N. I. Krikelis, "Modeling of multiple mobile manipulators handling a common deformable object," *J. Robot. Syst.*, vol. 15, pp. 599–623, 1998.

[16] K. Kosuge, T. Osumi, M. Sato, K. Chiba, and K. Takeo, "Transportation of a single object by two decentralized-controlled nonholonomic mobile robots," presented at the 1998 IEEE Int. Conf. Robotics Autom., Leuven, Belgium, 1998.

[17] M. Yamakita and J.-H. Suh, "Adaptive generation of desired velocity field for leader-follower type cooperative mobile robots with decentralized PVFC," in *Proc. 2001 IEEE Int. Conf. Robotics Autom.*, Seoul, Korea, vol. 4, 2001, pp. 3495–3502.

[18] P. S. Krishnaprasad and D. P. Tsakiris, "Oscillations SE(2)-snakes and motion control," presented at the IEEE 34th Conf. Decision Control, New Orleans, LA, 1995.

[19] J. P. Ostrowski, *The Mechanics and Control of Undulatory Robotic Locomotion*. Pasadena, CA: California Institute of Technology, 1995.

[20] G. Campion, G. Bastin, and B. D'Andrea-Novel, "Structural properties and classification of kinematic and dynamic models of wheeled mobile robots," *IEEE Trans. Robot. Autom.*, vol. 12, no. 1, pp. 47–62, Feb. 1996.

[21] F. G. Pin and M. Killough, "A new family of omnidirectional and holonomic wheeled plaforms for mobile robots," *IEEE Trans. Robot. Autom.*, vol. 10, no. 4, pp. 480–489, Aug. 1994.

[22] D. B. Reister and M. A. Unseren, "Position and contraint force control of a vehicle with two or more steerable drive wheels," *IEEE Trans. Robot. Autom.*, vol. 9, no. 6, pp. 723–731, Dec. 1993.

[23] S. V. Sreenivasan and K. J. Waldron, "Displacement analysis of an actively articulated wheeled vehicle configuration with extensions to motion planning on uneven terrain," *ASME J. Mech. Design*, vol. 118, pp. 312–317, 1996.

[24] K. H. Hunt, *Kinematic Geometry of Mechanisms*. Oxford: Clarendon, 1978.

[25] R. Murray, Z. Li, and S. Sastry, *A Mathematical Introduction to Robotic Manipulation*. Boca Raton, FL: CRC Press, 1993.

[26] J. M. Selig, *Geometric Fundamentals of Robotics*, 2nd ed. New York: Springer-Verlag, 2005.

[27] H. Bruyninckx and J. D. Schutter, "Unified kinetostatics for serial, parallel and mobile robots," presented at the 6th Int. Symp. Adv. Robot Kinematics, Strobl, Austria, 1988.

[28] C. P. Tang, R. M. Bhatt, and V. Krovi, "Decentralized kinematic control of payload transport by a system of mobile manipulators," presented at the 2004 IEEE Int. Conf. Robotics and Automation, New Orleans, LA, 2004.

[29] K. J. Waldron and K. H. Hunt, "Series-parallel dualities in actively coordinated mechanisms," *Int. J. Robot. Res.*, vol. 10, pp. 473–480, 1991.

[30] V. Kumar and K. J. Waldron, "Force distribution in closed kinematic chains," *IEEE Trans. Robot. Autom.*, vol. 4, no. 6, pp. 657–664, Dec. 1988.

[31] X. Yun and V. Kumar, "An approach to simultaneous control of trajectory and interaction forces in dual arm configurations," *IEEE Trans. Robot. Autom.*, vol. 7, no. 5, pp. 618–625, Oct. 1991.

[32] F. Firmani and R. P. Podhorodeski, "Force-unconstrained poses for a redundantly-actuated planar parallel manipulator," *Mech. Mach. Theory*, vol. 39, pp. 459–476, 2004.

[33] C. Gosselin and J. Angeles, "Singularity analysis of closed loop kinematic chains," *IEEE Trans. Robot. Autom.*, vol. 6, no. 3, pp. 281–290, Jun. 1990.

[34] F. Firmani and R. P. Podhorodeski, "Force-unconstrained poses for a redundantly-actuated planar parallel manipulator," *Mech. Mach. Theory*, vol. 39, pp. 459–476, 2004.

[35] R. M. Bhatt, "Formation motion planning for payload transport by modular wheeled mobile manipulators," M.S. thesis, Dept. Mech. Aero. Eng., State Univ. New York, Buffalo, 2003.

Chin Pei Tang (S'02) received the B.S. degree in mechanical engineering (with a minor in mathematics) in 2002, and the M.S. degree in mechanical engineering in 2004, both from the State University of New York, Buffalo, where he is currently pursuing the Ph.D. degree.

His research interests include cooperative robotics, modeling and control of mechanical and mechatronics systems.

Rajankumar M. Bhatt (S'02) received the B.Eng. degree in mechanical engineering from the M. S. University of Baroda, India, in 2000 and the M.S. degree in mechanical engineering from the State University of New York, Buffalo, in 2003, where he is currently pursuing the Ph.D. degree.

His research interests include cooperative mobile robots, graph theory, and dynamics of parallel the mechanical systems.

Michel Abou-Samah received the B.Eng. and M.Eng. degrees from McGill University, Montreal, QC, Canada, in 1999 and 2002, respectively, both in mechanical engineering.

Currently, he is an Application Engineer in the MSC Software Corporation, Ann Arbor, MI. His research was in the area of cooperative robot systems and virtual prototyping.

Venkat Krovi (S'97–M'99) received the M.S. and Ph.D. degrees from the University of Pennsylvania, Philadelphia, in 1995 and 1998, respectively, both in mechanical engineering.

In 2001, he joined the Department of Mechanical and Aerospace Engineering, State University of New York, Buffalo. His research interests include design, analysis, and prototyping of novel articulated mechanical systems.

Dr. Krovi was the recipient of the 2003 National Science Foundation CAREER Award.